A Linear Ion Trap Mass Spectrometer with Versatile Control and Data Acquisition for Ion/Ion Reactions

Matthew W. Soyk,[a,*] Qin Zhao,[a] R. S. Houk,[a,b] and Ethan R. Badman
[a] Department of Chemistry, Iowa State University, Ames, Iowa, USA
[b] Ames Laboratory, U.S. Department of Energy, Iowa State University, Ames, Iowa, USA

A linear ion trap (LIT) with electrospray ionization (ESI) for top-down protein analysis has been constructed. An independent atmospheric sampling glow discharge ionization (ASGDI) source produces reagent ions for ion/ion reactions. The device is also meant to enable a wide variety of ion/ion reaction studies. To reduce the instrument's complexity and make it available for wide dissemination, only a few simple electronics components were custom built. The instrument functions as both a reaction vessel for gas-phase ion/ion reactions and a mass spectrometer using mass-selective axial ejection. Initial results demonstrate trapping efficiency of 70% to 90% and the ability to perform proton transfer reactions on intact protein ions, including dual polarity storage reactions, transmission mode reactions, and ion parking. (J Am Soc Mass Spectrom 2008, 19, 1821–1831) © 2008 Published by Elsevier Inc. on behalf of American Society for Mass Spectrometry

Linear quadrupole ion traps (LITs) [1] have been a subject of recent interest, primarily because of their higher performance compared to 3D ion traps. Until recently, LITs were mainly used as ion storage devices or as collision cells for tandem mass spectrometry (MS/MS) preceding another type of mass analyzer (e.g., TOF [2, 3] or FT-ICR [4, 5]). Compared with 3D traps, LITs offer higher injection efficiency (<10% versus almost 100%, respectively) and, because of their larger volume, higher ion storage capacity, while still maintaining the ability to perform MS^n in a single device. More recently, two major innovations have led to widespread use of LITs as mass analyzers: radial [6] or axial [7] ejection methods. These LITs still have high trapping efficiency and storage capacity, with the added benefits of mass analysis in a single device [8].

For top-down protein analysis, linear and 3D ion traps cannot achieve the ultrahigh mass resolution and accuracy of FT-ICR [9] or Orbitrap instruments [10] necessary to resolve and unambiguously identify the isotopic distributions of highly multiply-charged ions. However, traps are well-suited to ion/ion reactions [11–13] like proton transfer to simplify the resulting complex, overlapping product ion spectra. Electron-transfer dissociation (ETD) [11] ion/ion reactions also provide an alternative tool for protein ion dissociation. Ion/ion reaction experiments have been carried out in both types of LITs, and although ETD capabilities are becoming more readily available on commercial ion traps, proton transfer reaction capabilities are not yet commercially available.

In addition, many researchers would like greater control and flexibility over instrumental parameters than is typically available in commercial devices, especially for fundamental experiments and development of new methods. Here we discuss the development of an electrospray ionization (ESI)-linear ion trap mass spectrometer that has been constructed to enable complete control over all functions of the device. Mass scanning by radial ejection requires machining an exit slit and channel in least one of the quadrupole rods. To simplify measurement of mass spectra and allow the future addition of subsequent components, e.g., ion mobility and time of flight analysis, this device is operated using mass-selective axial ejection (MSAE) [14]. Commercially available components were used primarily to reduce the complexity of the development and allow wide dissemination of this device to other researchers. Initial performance characteristics for MS and gas-phase ion/ion reactions are described, as well as future uses for this device in bioanalytical MS and as a source for ion mobility-TOF instruments.

McLuckey and coworkers have demonstrated the great value of commercial LITs with multiple pulsed ion sources, e.g., positive ESI for analyte ion formation plus negative ESI [15–18], negative atmospheric pressure chemical ionization [16, 18–21], or negative atmospheric sampling glow discharge ionization (ASGDI) [12, 22] for reagent ion formation. The present paper demonstrates the first work using a LIT with multiple

Address reprint requests to Dr. Ethan R. Badman, Hoffman-La Roche Inc., Nonclinical Safety, 340 Kingsland St., Nutley, NJ 07110, USA. E-mail: ethan.badman@roche.com
* Current address: LECO Corporation, 3000 Lakeview Ave., St. Joseph, MI 49085, USA.

1044-0305/08/$32.00
doi:10.1016/j.jasms.2008.08.020
Published online September 6, 2008
Received March 15, 2008
Revised August 16, 2008
Accepted August 23, 2008

ion sources interfaced through a turning quadrupole that has proven valuable with 3D ion traps [23, 24].

Experimental

Cytochrome *c*, ubiquitin and trypsin were purchased from Sigma-Aldrich (St. Louis, MO) and were used without further purification. Solutions of proteins were prepared at 20 to 30 μM in 1% aqueous acetic acid solutions for positive nano-ESI. Nano-ESI ionization emitters were pulled from glass capillaries (1.5 mm o.d., 0.86 mm i.d.) with a micropipette puller (model P-97; Sutter Instruments, Novato, CA). The nano-ESI voltage was +1 to +1.2 kV applied to a stainless steel wire through the back of the capillary. Perfluoro-1,3-dimethylcyclohexane (PDCH) was purchased from Sigma-Aldrich (St. Louis, MO) and was used as the reagent ion for proton transfer ion/ion reactions. The PDCH was ionized using an ASGDI source identical to that described by Zhao and coworkers [25].

Instrumentation

Figure 1 shows a schematic of the LIT with two ion sources: one ESI and one pulsed ASGDI source that are interfaced to the LIT through a quadrupole deflector. It should be noted that a third ion source could be added to the blank flange of the ion source cube shown in Figure 1. The LIT is a standard quadrupole mass filter modified to enable LIT functionality. Ions are detected with a conversion dynode/electron multiplier. Instrument control is via a commercially available ion trap controller and software. Figure 2 shows a schematic of how the ion trap controller and software communicate with and control all components of the LIT. Details about each part of the instrument are given below.

Vacuum System

The two ion sources and ion optics are housed in an 8 in. Conflat cube, and the LIT is housed in an 8 in. Conflat 5-way cross. One turbo pump (Turbo-V550 MacroTorr, 550 l/s N_2; Varian Inc., Palo Alto) is attached to the top of the cube that houses the ion sources, and a second, identical turbo pump is attached to the 5-way cross that houses the LIT. The turbo pump on the source cube is backed by a SD-301 mechanical pump (Varian Inc.), and the turbo pump on the LIT 5-way cross is backed by an E2M40 mechanical pump (BOC Edwards, Wilmington, MA). The chamber pressure is measured by a Micro-Ion Gauge (Helix Technology, Longmont, CO). The baseline pressure of the system is $\sim 5 \times 10^{-7}$ mbar.

Ion Sources and Ion Optics

Both ion sources have been described [24, 25]. Typical pressures in the ion source interface regions (i.e., behind the first 254 μm aperture to atmosphere and before the second 381 μm aperture to the high vacuum region) are 0.90 mbar and 0.80 mbar for the nano-ESI and ASGDI source, respectively. Each is pumped by a separate E2M40 mechanical pump. The pulsed ASGDI was initiated via a −400 V high voltage pulse supplied via a power supply (Model 556, Ortec, Oak Ridge, TN) through a fast pulser (model PVX4150; Directed Energy Inc., Fort Collins, CO). Voltages for the interfaces and the first three lenses are supplied via nine output power

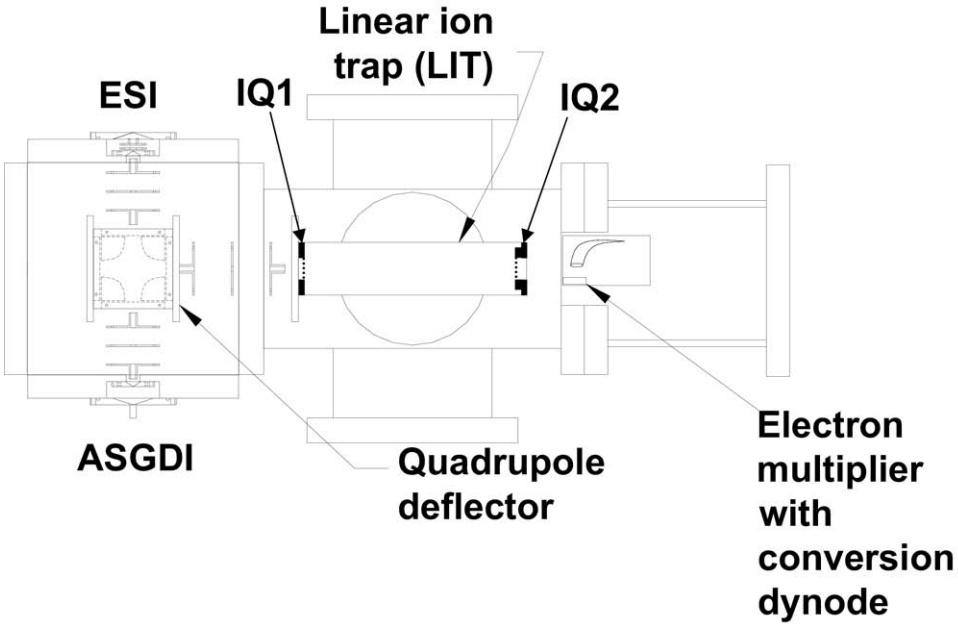

Figure 1. Instrument hardware schematic drawn to scale.

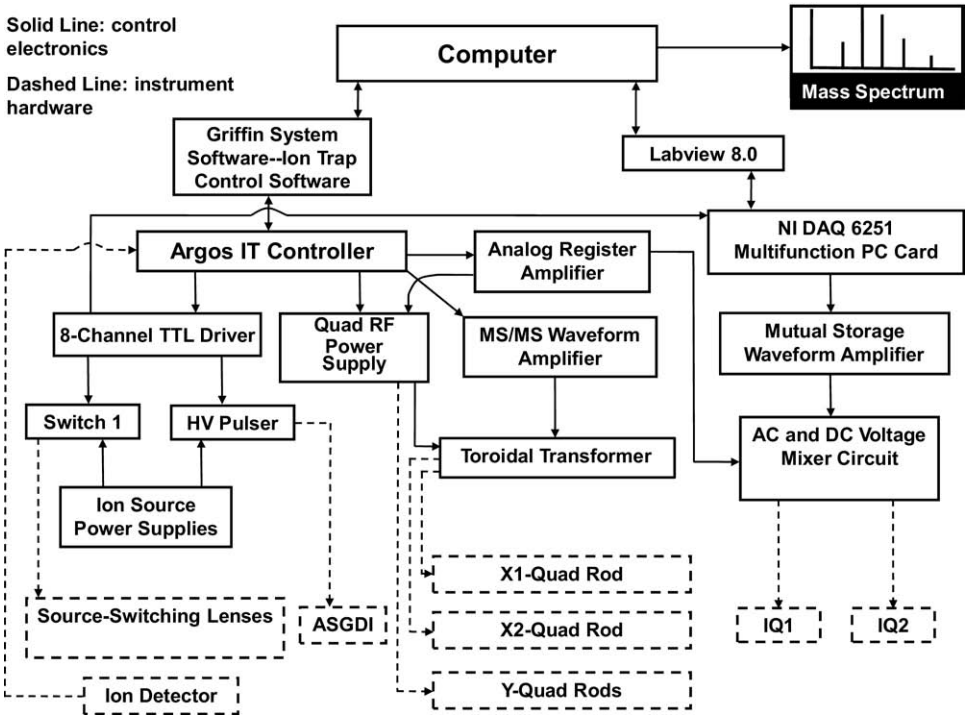

Figure 2. Instrument communication and control diagram.

supplies (model TD9500; Spectrum Solutions, Russelton, PA). The voltages on the quadrupole deflector (model 81,989; Extrel CMS, Pittsburgh, PA) and on the three lenses between the quadrupole deflector and the LIT are supplied via additional nine output power supplies, but are switched using a computer-controlled fast relay switch to enable ions from each source to be focused separately to the LIT as required. The ASGDI source is the default ion source. A single TTL trigger is used to switch the optics to allow ESI ions to enter the trap, and a second TTL trigger is used to pulse on the ASGDI discharge.

Linear Ion Trap

The LIT is a commercially available tri-filter quadrupole in a collision cell housing (r_0 = 4 mm; Extrel CMS, Pittsburgh, PA). The rf trapping voltage is supplied by a standard Extrel 300 W rf only power supply providing 3600 $V_{0\text{-}p}$ (pole to ground) at 880 kHz. To operate the quadrupole as an LIT, and perform MSAE [14] and MS/MS experiments, modifications were made to the quadrupole and rf electronics.

As described by Paul et al. [26], additional waveforms can be added to quadrupole rods to resonantly excite ions. Douglas and coworkers [2, 3] add dipolar excitation across a pair of opposite quadrupole rods to excite trapped ions for collision-induced dissociation and MS/MS. We implemented dipolar excitation by cutting the connections between one set of rods and adding an extra rf post and hole through the collision cell housing. To add the dipolar excitation voltage to the rf trapping voltage on one set of rods, a toroidal transformer was used. The toroid (model 5977003801; Fair-Rite, Wallkill, NY) was housed in a metal casing outside the vacuum chamber. The turn ratio between the primary and secondary was 1:1 using 16 turns of 22 gauge magnet wire (Belden Corporation, Chicago, IL). One of the outputs of the rf power supply was connected to the center tap of the secondary. The outputs of the secondary are then fed to the quadrupole rods through rf feedthroughs (model 810998; Extrel CMS, Pittsburgh, PA). One side of the primary was grounded, and the other was connected to the waveform generator.

The MSAE and MS/MS waveforms were generated from the ion trap controller. The original 5 $V_{0\text{-}p}$ was amplified to 35.5 $V_{0\text{-}p}$ using a custom amplifier (PA09 op-amp; Apex Microtechnology, Tucson, AZ) and applied to the primary of the transformer through a 50 Ω, 51 W resistor.

Two additional modifications to the quadrupole were required for effective trapping and *m/z* analysis. The post-filter was removed, and the pre-filter was shorted to the center quad section. The center rod section is the only section that is aligned with high precision. Therefore, removing the post-filter ensures that the fringe fields necessary for MSAE occur between the optimally-aligned center rod section and the exit aperture IQ2. Shorting the front and center sections together applies the full rf voltage to the entire trapping length and minimizes ion loss (from unequal potential well depths) as ions are trapped. This modification is especially important during charge reduction ion/ion reactions. As ions with a lower z—and correspondingly higher *m/z*—are formed, they will reside in increasingly

shallower potential wells. Without the full rf voltage on both the center and the pre-filter section, ions at high *m/z* are no longer trapped and are lost.

DC voltages (0–4 V) from an Argos ion trap controller (described in detail below) are amplified to ±200 V (PA97 op-amp, Apex Microtechnology), and controlled in the scan function with the ion trap controller. These dc voltages are applied to the entrance and exit lenses (IQ1, IQ2) and LIT rods (Q). The IQ1 and IQ2 lenses are 8 mm diameter and both are covered with nickel mesh (90% transparency, 70 lines per inch; InterNet Inc., Anoka, MN) on the interior side of the lenses. The distance from the IQ1 lens to the end of the quadrupole rods is ~5 mm. The IQ2 lens was modified to make the distance from the lens to the end of the quadrupole rods ~2 mm.

To fully resonate the rf power supply after adding the toroidal transformer and changing the arrangement of the quad sections, the overall capacitance of the load was reduced by the following measures. (1) The original rf cable between the power supply and the transformer was shortened by 53 cm, from 166.3 cm to 113.3 cm. (2) The magnet wire used in the toroidal transformer was covered with Teflon tubing (1.7 mm o.d.., 1.1 mm i.d.). (3) A 3 pF capacitor in the rf power supply near the output on both the toroid and non-toroid sides was removed. (4) The tap of the rf coil was moved to remove 2.25 turns on the toroid side and 1 turn on the non-toroid side. By performing these steps, the power supply could generate nearly the maximum original rf voltage, as read by the internal feedback circuit.

To make sure similar rf voltages were applied to each of the quadrupole rods, two duplicate rf detector circuits identical to those used by the Extrel power supply were built. These devices convert the rf voltage to a current that can be read with a digital multimeter. Using this method, the two sides of the rf output could be tuned to be within 1.99% ± 0.25% of each other, limited by the accuracy of the digital multimeter.

The nitrogen buffer gas pressure in the LIT is adjusted using a variable leak valve (model 203; Helix Technology, Longmont, CO) and measured by the pressure in the main chamber using the Micro-Ion Gauge. During a typical experiment, the chamber pressure is maintained at $\sim 1.3 \times 10^{-4}$ mbar with both sources open and nitrogen gas added to the LIT. Of course, the pressure inside the LIT is higher than that measured by the ion gauge. From the sizes of the IQ1 and IQ2 lenses (8 mm diameter), the 90% mesh covering the lenses, the measured pressure in the vacuum chamber (1.3×10^{-4} mbar), and the pumping speed (550 l/s), the pressure inside the LIT is estimated to be 5×10^{-3} mbar, assuming effusive flow out of IQ1 and IQ2.

Mass spectra are acquired using MSAE by ramping the rf voltage while applying a dipolar resonance excitation frequency and a small, constant, repulsive voltage to IQ2 (typically +1 to +3 V for positive ions), while the dc voltage on the LIT rods is kept at ground. Ejected ions are detected with an electron multiplier with conversion dynode (402A-H; Detector Technology Inc., Palmer, MA). Scans were measured only in the forward direction, from low *m/z* to high *m/z*.

Modifications for Ion/Ion Reactions with Dual Polarity Trapping

To perform dual polarity storage mode ion/ion reactions, and store both positive and negative ions simultaneously, AC voltages are applied to IQ1 and IQ2 during PDCH injection and subsequent reaction time [11]. This axial trapping voltage is generated via a multifunction PC card (model 6251; National Instruments, Austin TX) with custom software written in Labview 8.0. The frequency and amplitude are set in the software—and are, therefore, fixed during an experiment—and the waveform is switched on and off via a TTL trigger (1 μs delay). The initial 0–5 $V_{0\text{-}p}$ sine wave is amplified via a custom amplifier (PA90; Apex Microtechnology, Tucson, AZ) up to 175 $V_{0\text{-}p}$ and split into two 180° out-of-phase signals. The ac voltages are added to the dc voltage for IQ1 and IQ2 using a simple mixer circuit. Typically, the waveform is applied at 100 kHz, with an amplitude of ~50 $V_{0\text{-}p}$, empirically determined to minimize ion loss during the reaction period. The amplitude and frequency of this waveform are lower than those used by McLuckey and coworkers [17].

In the first scan function segment of a dual polarity trapping ion/ion reaction, three processes are done simultaneously; the dc potentials on the IQ1 and IQ2 lenses are set to 0V (the same potential as the quadrupole rods), the axial trapping waveform is turned on, and the ASGDI source is pulsed on. In the second segment, the ASGDI source is turned off, and the analyte and reagent ions are allowed to react. To end the reaction, the axial trapping waveform is turned off and the dc potentials on the IQ1 and IQ2 lenses are, simultaneously, set to repel (i.e., trap) the positive analyte ions, while excess negative reagent ions are ejected out both ends of the LIT.

Ion/Ion Reactions in Transmission Mode and Ion Parking

Ion/ion reactions in transmission mode have been described previously [15, 19]. Transmission mode reactions are enabled by trapping the analyte ions using small repulsive dc voltages (typically 2 to 5 V) on the IQ1 and IQ2 lenses and passing the reagent ions, continuously generated by the ASGDI source during the reaction time, through the population of trapped analyte ions. Any unreacted reagent ions pass completely through the LIT and are lost. Ending the transmission mode reactions simply requires turning off the ASGDI source, thus turning off the reagent ion beam. The reaction product ions remain trapped in the LIT because they are the same polarity as the unreacted analyte ions.

Ion/ion reactions carried out using this method do not require the use of the axial trapping waveform, and there is only one scan segment for the reaction period. Therefore, the scan function for transmission mode ion/ion reactions is simpler than that for dual polarity trapping ion/ion reactions. Additionally, the electronics required to add the dual polarity trapping waveform to the containment lenses are not required, making the LIT hardware for transmission mode reactions much simpler than that for dual polarity storage mode reactions.

Ion parking [27] is a technique that was developed by McLuckey and coworkers in which the rate of reaction for ions at a single *m/z* value [27] or multiple *m/z* values [28, 29] are inhibited selectively. Increasing the relative velocity of reactant ions, which reduces the ion/ion reaction capture cross section, during an exothermic ion/ion reaction decreases the rate of reaction between those ions [27]. To enable ion parking, a low amplitude auxiliary sine wave (initially $\sim 1V_{0\text{-}p}$, ~50 kHz for the ions chosen here) is added to the x-rods of the LIT during the ion/ion reaction period. The auxiliary sine wave resonantly excites a particular product ion formed during the ion/ion reaction. The frequency and amplitude of the sine wave are chosen so that the ions being parked are excited enough to inhibit the reaction rate but not so much that they are ejected from the LIT. These values are fine-tuned empirically to produce the desired results. As the reaction proceeds and the ion chosen to be parked is formed, it is resonantly excited by the applied auxiliary sine wave. The velocity of the excited ion relative to the reagent anion increases, thereby reducing its ion/ion reaction rate and minimizing further reaction. For the proton transfer ion/ion reactions on intact protein ions studied here, the result of an ion parking experiment is the concentration of most of the ions into a single charge state below that of the original ions.

Electronics

An Argos ion trap controller (Griffin Analytical Technology, West Lafayette, IN) controls the entire instrument and acquires data. The scan function is generated by the Argos software. TTL pulses ("relays") trigger the ASGDI source, switch the fast relay switch to enable injection of oppositely-charged ions, and toggle on the ion/ion trapping voltage. The two waveform outputs control the rf level (0–10 V control 0-3600 $V_{0\text{-}p}$ of rf) and generate MS/MS waveforms, respectively. Different from previous versions of the Argos software, this version provides time-dependent dc voltages (0–4 V "registers") that control the voltages applied to IQ1, IQ2, and the LIT rods.

Data are acquired using the Argos data input (at a 250 kHz sampling rate) but, as a result, the data acquisition time is limited to 250 ms or less. Primarily, this limits the ability to perform slow mass scans over a wide mass range.

Results and Discussion

LIT Performance

Initial characterization of the LIT includes determination of trapping efficiency, ion capacity, mass analysis efficiency, and measurement of mass accuracy. To determine the trapping efficiency, ions are gated into the trap for a specified time, cooled, and then dumped to the detector (in a non-mass selective manner) by dropping the IQ2 voltage. The response from the trapped ions is then compared to the response acquired during operation of the quadrupole as an rf-only ion guide for the same time as the trap fill time at the same rf level.

Table 1 shows trapping efficiencies at four different fill times for positive ions of cytochrome *c* and trypsin generated by ESI. Efficiencies average 83% with a range from 68% to 92%. These values agree with those determined previously from other LIT instruments [6, 7].

Figure 3 shows a plot of total ion current (TIC) versus LIT fill time for cytochrome *c* that is used to measure the ion capacity of the LIT. The response is nearly linear from 5 to 40 ms, after which the signal levels off. The ion current on IQ1 was then measured—with all LIT and ion detector voltages turned off—using a picoammeter (model 6485; Keithley Instruments, Cleveland, OH) to determine the real number of ions delivered to the trap. It was assumed that the rate of ions that strike the wires of the Ni mesh covering IQ1, after accounting for the 90% transmission, approximates the rate at which ions are delivered to the LIT during the fill step of a trapping experiment. Using the average measured ion current from the IQ1 Ni mesh (7.97 pA), the correction for the 90% transmission, the fill time at which the response levels off (40 ms), the measured trapping efficiency (83%), and the average charge state of the cytochrome *c* ions used for the measurement (+8.5), it was determined that $\sim 1.9 \times 10^6$ ions can be trapped in the LIT. The maximum total charge in the LIT is thus $\sim 1.6 \times 10^7$ charges. To avoid space charge effects, the LIT is not filled to this capacity during normal operation.

Mass Spectra

A typical protein mass spectrum taken using MSAE is shown in Figure 4. The inset of Figure 4 shows the peak shape for the +9 charge state of cytochrome *c*. This peak has a full-width at half maximum (fwhm) of 1.11 Th, corresponding to a resolution of 1230. The measured

Table 1. Trapping efficiency and MSAE efficiency at various ion fill times for cytochrome *c* and trypsin ions. Uncertainties represent the standard deviations of four to six such measurements

Fill time (ms)	Trapping efficiency (%)	MSAE efficiency (%)
5	68.9 ± 11.1	9.6 ± 1.8
10	85.3 ± 4.6	7.7 ± 1.6
15	84.9 ± 8.2	6.4 ± 1.7
20	92.0 ± 4.8	5.1 ± 0.86

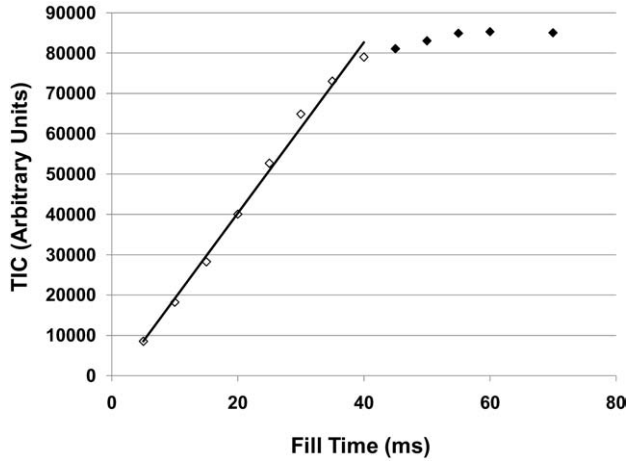

Figure 3. Plot of total ion current versus fill time used to measure the ion capacity of the LIT.

fwhm from the LIT is about 1.4× larger than the calculated width of the isotopic envelope (0.77 Th, fwhm). Of course, resolving the isotopic distribution of this peak requires resolution in excess of ~18,000 (50% valley).

Table 2 shows the trapping voltages and ejection conditions used to take the spectrum shown in Figure 4. These operating conditions are typical for mass spectra taken with the LIT. The spectrum in Figure 4 shows adduct or impurity peaks at 54, 90, and 130 Da above each protein peak. The scan function used to generate this spectrum includes a heating ramp in which a 1.9 $V_{0\text{-}p}$, 150 kHz sine wave is applied to the x-rods while the rf amplitude is ramped to bring the protein ions into resonance with the applied sine wave. Thus the ions are heated, and the adducts/impurities are dissociated. Without this heating ramp, the overall protein peak is very wide, encompassing the protein and all the adduct/impurity ions into a single wide peak. The adduct/impurity peaks could not be totally eliminated without severely reducing the intensity of the protein peak. It should also be noted that these same adduct peaks are seen from the same protein samples on another home-built MS in our lab [25].

The mass analysis efficiency is measured using a similar procedure as the trapping efficiency measurement. Protein ions are gated into the LIT for a specified time, cooled, and non-mass selectively emptied to the detector by dropping the potential on IQ2. In a second experiment, protein ions are gated into the LIT for the same specified time—ensuring that the number of ions inside the trap is approximately the same for both experiments—cooled, and mass analyzed using MSAE. The ratio of the TIC of the ions ejected under MSAE conditions to the TIC of all the ions trapped (measured by non-mass selectively ejecting ions) yields an average measured MSAE efficiency of 7.4% ± 2.2%. Using the average measured MSAE efficiency and the overall length of the LIT (18.7 cm), it was calculated that the extraction region is 18.7 × 0.074 = 1.4 cm long. The measured efficiency and extraction region length are less than the results obtained by Hager [7] at similar LIT pressure. Conversely, the measured MSAE efficiency is slightly higher than recent results obtained by Douglas and coworkers [30]. Our measured efficiency may be higher due to higher pressure in our LIT and the lower

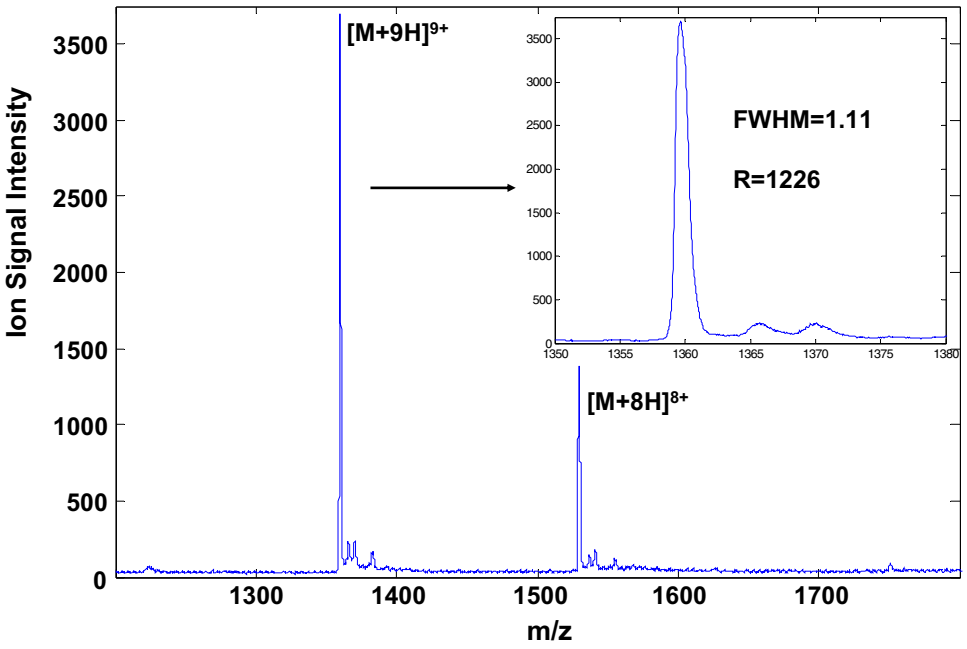

Figure 4. Cytochrome *c* mass spectrum. A heating ramp (100 ms, 540 to 1260 $V_{0\text{-}p}$ rf, 1.9 $V_{0\text{-}p}$, 150 kHz sine wave) reduced the intensity of the adduct peaks that are visible at 54, 90, and 130 Da above each protein peak.

Table 2. Typical LIT conditions used to trap and eject ions over 1100–1800 *m/z* range

Scan step	IQ1 (V)	IQ2 (V)	RF amplitude ($V_{0\text{-}p}$)	Resonance amplitude ($V_{0\text{-}p}$)	Resonance frequency (kHz)	Scan rate (Da/s)
Fill (10–20 ms)	−10	10	360	—	—	—
Cool (30 ms)	10	10	360	—	—	—
Heating ramp (100 ms)	10	10	540 to 1260	1.9	150 (q = 0.46)	12,300
Cool (30 ms)	10	10	1080	—	—	—
Mass scan (250 ms)	10	2	1080 to 1800	2.8 to 3.7	275 (q = 0.75)	3000

spectral resolution than in the results recorded by Douglas.

Table 1 shows MSAE efficiency measurements for different fill times of cytochrome *c* and trypsin. The data shows that as fill time increases the MSAE efficiency decreases. Space charge effects may degrade the MSAE efficiency at longer fill times.

Mass accuracy was determined by spraying a 50:50 mixture of cytochrome *c* and ubiquitin. The peak maxima for $[M + 9H]^{9+}$ and $[M + 8H]^{8+}$ of the cytochrome *c* ions (*m/z* ~1360 and 1530) were used to calibrate the *m/z* axis and the *m/z* at the peak maxima of $[M + 7H]^{7+}$ and $[M + 6H]^{6+}$ ions of ubiquitin (*m/z* ~ 1224 and 1429) were measured. These solvent and source conditions yield few ions from cytochrome c in charge states above +9. Measured mass accuracies range from 900 to 2200 ppm. The accuracy limitations are likely due to voltage stability for the rf trapping voltage, resonance excitation voltage, and/or IQ2 dc voltage. The use of calibrant ions in a *m/z* window that spans that of the analyte may also improve mass measurement accuracy.

To illustrate the performance of the LIT as a mass analyzer at moderate *m/z* values, a spectrum of the PDCH reagent anions from the glow discharge source is shown in Figure 5a. These ions are a mixture of $[M - F]^-$ and $M^{\cdot-}$ [31]. The inset shows the peak shape and resolution for the $[M - F]^-$ ion. The ^{13}C isotope peak is cleanly resolved from the main peak at *m/z* 381. The nominal resolution value is $m/\Delta m$ = ~1080 at fwhm.

It should be noted that nonlinear resonance ejection peaks can be seen under certain conditions. These "ghost peaks" [32] occur at a q_z value of 0.64 ($\beta = 0.5$ or 220 kHz in this system) consistent with octopolar field ejection [33]. Use of resonance ejection frequencies near this nonlinear resonance can produce asymmetric or split peaks. Therefore, the resonance ejection frequency is selected to avoid this nonlinear resonance value.

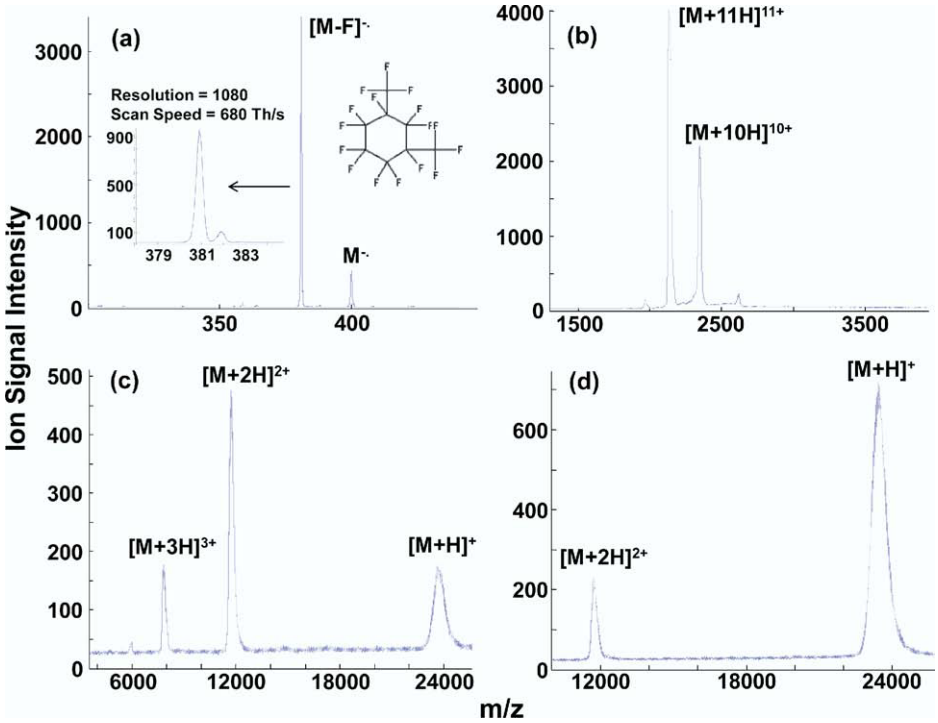

Figure 5. Mass spectra taken from dual polarity storage mode proton transfer ion/ion reactions of intact protein trypsin. (**a**) Negative ion mode spectrum of the proton transfer reagent ion, PDCH. (**b**) Pre-ion/ion reaction spectrum of trypsin ions generated directly from ESI. (**c**) Post-ion/ion reaction spectrum of ions shown in (**a**) and (**b**) with a 15 ms PDCH fill and 100 ms reaction. (**d**) Post-ion/ion reaction spectrum of ions shown in (**a**) and (**b**) with a 20 ms PDCH fill and 100 ms reaction.

Dual Polarity Trapping Mode Ion/Ion Reactions

The application of the dual polarity storage mode waveform used for ion/ion reactions is similar to that described previously [11]. The dual polarity storage mode proton transfer ion/ion reaction scan function consists of the following steps: filling the trap with protein cations, a cooling segment, a heating ramp to eliminate adduct peaks from the protein, another cooling segment, a PDCH fill segment, an additional reaction segment, a final cooling segment, and mass analysis.

The results of such a dual polarity storage mode reaction between trypsin positive ions and negative PDCH ions are shown in Figure 5. The mass spectrum of the trypsin ions formed directly from ESI is shown in Figure 5b. The main ions observed under these sample and source conditions are the $[M + 11H]^{11+}$ and $[M + 10H]^{10+}$ charge states, with small amounts of the $[M + 9H]^{9+}$ and $[M + 12H]^{12+}$ charge states. In the subsequent parts of Figure 5, the LIT is also filled with negative ions from PDCH (Figure 5a) for either 15 or 20 ms. The PDCH fill step is followed by a period of dual polarity storage where the positive trypsin ions and negative PDCH ions are allowed to react further. The amplitude of the LIT rf voltage during the ion/ion reaction periods is set at 360 $V_{0\text{-}p}$, leaving the most abundant PDCH ion ($[M - F]^-$) at q = 0.74. This amplitude rf was empirically chosen to maximize the amount of high mass product ions that are trapped while still trapping the PDCH reagent ion. The dual polarity trapping waveform added to IQ1 and IQ2 during the ion/ion reaction period is a 100 kHz sine wave with an amplitude of 50 $V_{0\text{-}p}$.

A PDCH fill time of 15 ms and additional reaction time of 100 ms converts the trypsin ions shown in Figure 5b to the $[M + 3H]^{3+}$, $[M + 2H]^{2+}$, and $[M + H]^+$ charge states (Figure 5c). Continuing the reaction for times in excess of 100 ms does not result in further conversion of trypsin ions to lower charge states (data not shown). Thus, all the PDCH anions that were trapped in a 15 ms fill time have been reacted after a 100 ms reaction.

Figure 5c results when this dual polarity storage mode reaction experiment is repeated with a PDCH fill time of 20 ms and an additional reaction time of 100 ms. The multiply charged trypsin ions from Figure 5b are converted to primarily $[M + H]^+$, m/z = ~24,000. The fwhm of the peak for this ion is 673 Th, and the resolution is 34. At this time, the $[M + H]^+$ ion of trypsin is the highest m/z ion created and ejected from this LIT.

This trypsin $[M + H]^+$ ion at $m/z \sim 24{,}000$ was observed by resonance ejection using a 35 kHz sine wave added to the LIT rods during the mass scan. The amplitude of this resonant excitation sine wave was

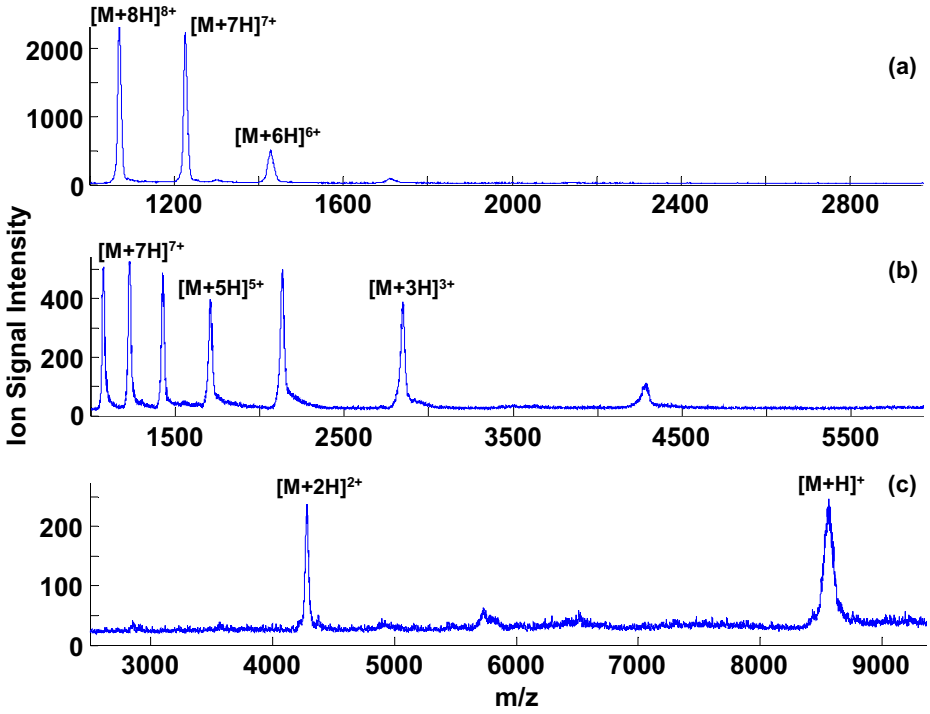

Figure 6. Mass spectra taken from transmission mode proton transfer ion/ion reactions of intact protein ubiquitin. (**a**) Pre-ion/ion reaction spectrum of ubiquitin ions generated directly from ESI. (**b**) Mass spectrum resulting from a transmission mode proton transfer ion/ion reaction enabled by passing PDCH anions through the population of trapped ubiquitin ions from (**a**) for 40 ms. (**c**) Mass spectrum resulting from a transmission mode proton transfer ion/ion reaction enabled by passing PDCH anions through the population of trapped ubiquitin ions from (**a**) for 70 ms.

ramped from 8.9 to 24.8 $V_{0\text{-}p}$. The dc voltage on the IQ2 lens was set to be 2.5 V relative to the LIT rod bias (0 V dc). The resonance ejection method provides a means to measure large protein ions in low charge states after charge reduction reactions, although the spectral resolution is generally mediocre; e.g., Xia et al. report a resolution of 180 fwhm for singly charged horse heart myoglobin at *m/z* 17,000 [12].

Transmission Mode Ion/Ion Reactions

Results of proton transfer ion/ion reactions of multiply charged ubiquitin cations with PDCH anions are shown in Figure 6. During the transmission mode reaction period, the amplitude of the LIT rf voltage is set at 360 $V_{0\text{-}p}$, leaving the most abundant PDCH ion ($[M - F]^-$) at q = 0.74, an equivalent value to dual polarity trapping mode experiments. Also, injecting reagent anions at high q-values results in the greatest spatial overlap between the analyte and reagent ions, maximizing the ion/ion reaction rate [15, 19]. The dc voltages on IQ1 and IQ2 were set at 3 V repulsive relative to the rod dc bias (0 V).

Figure 6a shows the mass spectrum of ubiquitin obtained directly from ESI. The solution and ESI source conditions yield ubiquitin ions primarily in the $[M + 6H]^{6+}$ to $[M + 8H]^{8+}$ charge states. As shown in Figure 6b, transmission mode reaction with PDCH anions for 40 ms converts approximately half these ions to the $[M + 3H]^{3+}$ to $[M + 5H]^{5+}$ charge states, while the other half of the ions are lost. Extending the reaction period to 70 ms converts the ions to roughly equal amounts of $[M + H]^+$ and $[M + 2H]^{2+}$ (Figure 6c). In the latter experiment, continuing the reaction long enough to reduce the ions to $[M + H]^+$ and $[M + 2H]^{2+}$ results in peaks that are only ~10% as high as those for the original spectrum. Most of this is due to ion losses from the ion/ion reaction, but some is attributed to loss in detector response for ions with lower charge. The same effect is seen in Figure 5 for trypsin in dual polarity storage mode. Others also report ion losses of similar magnitude as a consequence of ion/ion reactions, in either 3d ion traps or LITs [15, 27].

Ion Parking

Ion parking should alleviate some of the ion losses during proton transfer reactions. Results from such an experiment involving cytochrome *c* ions are shown in Figure 7. Here the vertical scales have been kept constant so the signals can be compared more easily. The pre-ion/ion reaction spectrum of cytochrome *c* (Figure 7a) shows mostly the $[M + 9H]^{9+}$ and $[M + 8H]^{8+}$ charge states. A transmission mode reaction enabled by passing PDCH anions through the population of

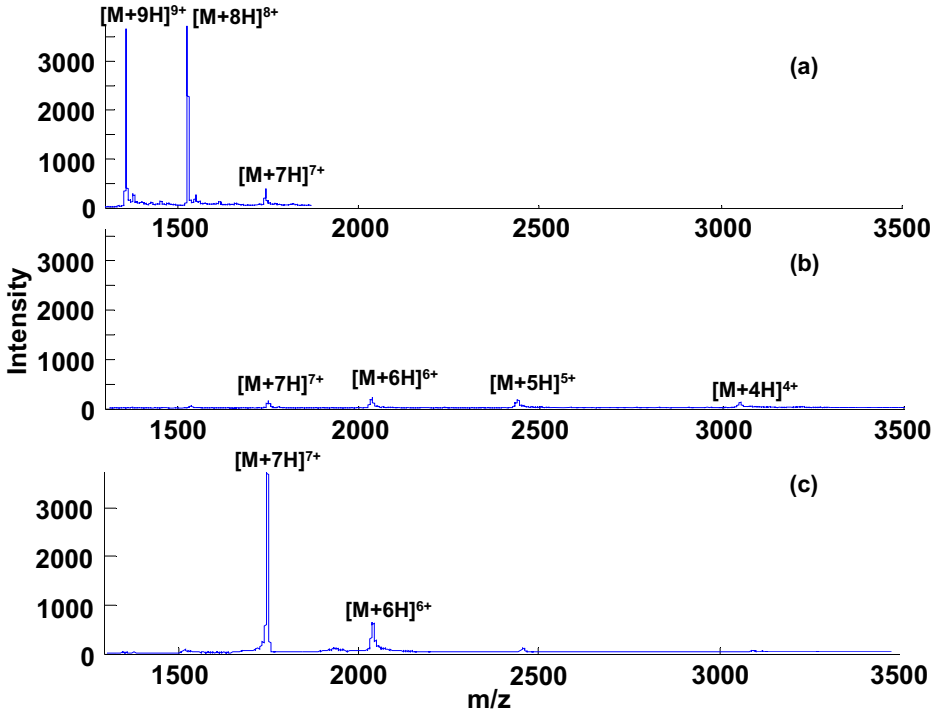

Figure 7. Mass spectra taken from an ion parking experiment during a transmission mode proton transfer ion/ion reaction. (**a**) Pre-ion/ion reaction spectrum of cytochrome *c* ions generated directly from ESI. (**b**) Mass spectrum resulting from a transmission mode proton transfer ion/ion reaction enabled by passing PDCH anions through the population of trapped cytochrome *c* from (**a**) for 20 ms. (**c**) Mass spectrum resulting from a transmission mode proton transfer ion/ion reaction enabled by passing PDCH anions through the population of trapped cytochrome *c* ion from (**a**) for 20 ms, during which a 1.8 $V_{0\text{-}p}$, 42 kHz sine wave was added to the x-rods of the LIT, "parking" the $[M + 7H]^{7+}$ ion.

trapped cytochrome *c* ions for 20 ms yields a variety of peaks from $[M + 7H]^{7+}$ to $[M + 4H]^{4+}$, all with low abundances (Figure 7b). In Figure 7c, a waveform selected to excite the $[M + 7H]^{7+}$ ion (1.8 $V_{0\text{-}p}$ and 42 kHz) is applied to the x-rods during the transmission mode reaction period. With ion parking enabled, most of the resulting product ions remain in the $[M + 7H]^{7+}$ charge state; about 20% react further to form $[M + 6H]^{6+}$ and a small amount of $[M + 5H]^{5+}$. The signal in the $[M + 7H]^{7+}$ charge state after the reaction with ion parking (Figure 7c) is about half of the total ion signal present in the $[M + 9H]^{9+}$ and $[M + 8H]^{8+}$ charge states created directly from the ESI source (Figure 7a), which is a much less severe compromise of signal than that shown for ion/ion reactions without ion parking in Figures 5 and 6.

Conclusions

A research-grade LIT with multiple ion sources was designed and constructed using primarily commercially available components. Preliminary experiments show that its trapping efficiency is similar to that of commercial LITs and its performance as a mass spectrometer is good compared to the theoretical peak width of the cytochrome *c* charge states. Ion/ion reaction capabilities in both dual polarity storage mode and transmission mode were also demonstrated. The device operates under versatile computer control that should facilitate application to various schemes for ion/ion reactions and other ways to manipulate ions.

Future plans for this instrument include: enabling top-down protein analysis, including both collision induced dissociation followed by proton transfer ion/ion reactions as well as electron-transfer dissociation (ETD) [11]. A second plan for this instrument is writing a data acquisition program in Labview 8.0 to enable data acquisition with the National Instruments multifunction PC card mentioned earlier. This modification should allow measurement times longer than the 250 ms limit of the Argos data acquisition system. Another future use for this instrument is to replace the 3d ion trap as the source for an ion mobility-time-of-flight (IMS-TOF) device that was built in our lab [25].

Acknowledgments

The authors acknowledge the following individuals: Chris Doerge and Don Douglas for helpful discussions and advice on construction of the toroidal transformer; Gregg Schieffer for help with testing of the custom electronics; Dick Egger, the late Steve Lee, and Terry Soseman (ISU Chemistry Machine Shop) for precision machining; Charlie Burg (Ames Lab ESG) for vacuum welding; Lee Harker (Ames Lab ESG) and Chuck Reese (ISU Chemistry) for custom electronics design, construction, and maintenance; Brian Regel and Brian Lippert at Extrel CMS for helpful discussion about the rf electronics; Brent Knecht, Brent Rardin, and Mitch Wells (Griffin Analytical Technologies) for development and testing of the LIT software; Scott McLuckey for the plans for the computer-controlled fast relay switch; and James Hager, MDS SCIEX, for discussions about improving the performance of the LIT.

The authors acknowledge funding for this work by a grant from the Iowa State University Vice Provost for Research. M.W.S. acknowledges Extrel CMS for the Richard A. Schaeffer Memorial Travel Award to present this work at the 2006 ASMS Conference. M.W.S. also acknowledges the Velmer A. and Mary K. Fassel Fellowship (Iowa State University, 2006–2007), the ConocoPhillips Fellowship (Iowa State University, 2006–2007), and the GAANN Fellowship (Iowa State University, 2008) for financial support.

References

1. Douglas, D. J.; Frank, A. J.; Mao, D. M. Linear ion traps in mass spectrometry. *Mass Spectrom. Rev.* **2005,** *24*, 1–29.
2. Campbell, J. M.; Collings, B. A.; Douglas, D. J. A new linear ion trap time-of-flight system with tandem mass spectrometry capabilities. *Rapid Commun. Mass Spectrom.* **1998,** *12*, 1463–1474.
3. Collings, B. A.; Campbell, J. M.; Mao, D. M.; Douglas, D. J. A combined linear ion trap time-of-flight system with improved performance and MSn capabilities. *Rapid Commun. Mass Spectrom.* **2001,** *15*, 1777–1795.
4. Harkewicz, R.; Belov, M. E.; Anderson, G. A.; Pasa-Tolic, L.; Masselon, C. D.; Prior, D. C.; Udseth, H. R.; Smith, R. D. ESI-FTICR mass spectrometry employing data-dependent external ion selection and accumulation. *J. Am. Soc. Mass Spectrom.* **2002,** *13*, 144–154.
5. Syka, J. E. P.; Marto, J. A.; Bai, D. L.; Horning, S.; Senko, M. W.; Schwartz, J. C.; Ueberheide, B.; Garcia, B.; Busby, S.; Muratore, T.; Shabanowitz, J.; Hunt, D. F. Novel linear quadrupole ion trap/FT mass spectrometer: Performance characterization and use in the comparative analysis of histone H3 post-translational modifications. *J. Proteome Res.* **2004,** *3*, 621–626.
6. Schwartz, J. C.; Senko, M. W.; Syka, J. E. P. A two-dimensional quadrupole ion trap mass spectrometer. *J. Am. Soc. Mass Spectrom.* **2002,** *13*, 659–669.
7. Hager, J. W. A new linear ion trap mass spectrometer. *Rapid Commun. Mass Spectrom.* **2002,** *16*, 512–526.
8. Jonscher, K. R.; Yates, J. R. The quadrupole ion trap mass spectrometer—a small solution to a big challenge. *Anal. Biochem.* **1997,** *244*, 1–15.
9. Reid, G. E.; McLuckey, S. A. 'Top down' protein characterization via tandem mass spectrometry. *J. Mass Spectrom.* **2002,** *37*, 663–675.
10. Hu, Q. Z.; Noll, R. J.; Li, H. Y.; Makarov, A.; Hardman, M.; Cooks, R. G. The Orbitrap: a new mass spectrometer. *J. Mass Spectrom.* **2005,** *40*, 430–443.
11. Syka, J. E. P.; Coon, J. J.; Schroeder, M. J.; Shabanowitz, J.; Hunt, D. F. Peptide and protein sequence analysis by electron transfer dissociation mass spectrometry. *Proc. Natl. Acad. Sci. U.S.A.* **2004,** *101*, 9528–9533.
12. Xia, Y.; Wu, J.; McLuckey, S. A.; Londry, F. A.; Hager, J. W. Mutual storage mode ion/ion reactions in a hybrid linear ion trap. *J. Am. Soc. Mass Spectrom.* **2005,** *16*, 71–81.
13. Stephenson, J. L.; McLuckey, S. A. Simplification of product ion spectra derived from multiply charged parent ions via ion/ion chemistry. *Anal. Chem.* **1998,** *70*, 3533–3544.
14. Londry, F. A.; Hager, J. W. Mass selective axial ion ejection from a linear quadrupole ion trap. *J. Am. Soc. Mass Spectrom.* **2003,** *14*, 1130–1147.
15. Liang, X. R.; McLuckey, S. A. Transmission mode ion/ion proton transfer reactions in a linear ion trap. *J. Am. Soc. Mass Spectrom.* **2007,** *18*, 882–890.
16. Liang, X. R.; Han, H. L.; Xia, Y.; McLuckey, S. A. A pulsed triple ionization source for sequential ion/ion reactions in an electrodynamic ion trap. *J. Am. Soc. Mass Spectrom.* **2007,** *18*, 369–376.
17. Xia, Y.; Liang, X. R.; McLuckey, S. A. Pulsed dual electrospray ionization for ion/ion reactions. *J. Am. Soc. Mass Spectrom.* **2005,** *16*, 1750–1756.
18. Xia, Y.; Chrisman, P. A.; Erickson, D. E.; Liu, J.; Liang, X. R.; Londry, F. A.; Yang, M. J.; McLuckey, S. A. Implementation of ion/ion reactions in a quadrupole/time-of-flight tandem mass spectrometer. *Anal. Chem.* **2006,** *78*, 4146–4154.
19. Liang, X. R.; Hager, J. W.; McLuckey, S. A. Transmission mode ion/ion electron-transfer dissociation in a linear ion trap. *Anal. Chem.* **2007,** *79*, 3363–3370.
20. Liang, X. R.; Xia, Y.; McLuckey, S. A. Alternately pulsed nanoelectrospray ionization/atmospheric pressure chemical ionization for ion/ion reactions in an electrodynamic ion trap. *Anal. Chem.* **2006,** *78*, 3208–3212.
21. Han, H. L.; Xia, Y.; McLuckey, S. A. Ion trap collisional activation of c and z(center dot) ions formed via gas-phase ion/ion electron-transfer dissociation. *J. Proteome. Res.* **2007,** *6*, 3062–3069.
22. Wu, J.; Hager, J. W.; Xia, Y.; Londry, F. A.; McLuckey, S. A. Positive ion transmission mode ion/ion reactions in a hybrid linear ion trap. *Anal. Chem.* **2004,** *76*, 5006–5015.

23. Wells, J. M.; Chrisman, P. A.; McLuckey, S. A. "Dueling" ESI: Instrumentation to study ion/ion reactions of electrospray-generated cations and anions. *J. Am. Soc. Mass Spectrom.* **2002,** *13*, 614–622.
24. Badman, E. R.; Chrisman, P. A.; McLuckey, S. A. A quadrupole ion trap mass spectrometer with three independent ion sources for the study of gas-phase ion/ion reactions. *Anal. Chem.* **2002,** *74*, 6237–6243.
25. Zhao, Q.; Soyk, M. W.; Schieffer, G. M.; Houk, R. S.; Badman, E. R.; Fuhrer, K.; Gonin, M. An ion trap-ion mobility-time of flight mass spectrometer with three ion sources for ion/ion reactions. *J. Am. Soc. Mass Spectrom.* **2008**, unpublished.
26. Paul, W.; Reinhard, H. P.; Vonzahn, U. The electric mass filter as mass spectrometer and isotope separator. Zeitschrift fur Physik. 1958, 152, 143–182.
27. McLuckey, S. A.; Reid, G. E.; Wells, J. M. Ion parking during ion/ion reactions in electrodynamic ion traps. *Anal. Chem.* **2002,** *74*, 336–346.
28. Chrisman, P. A.; Pitteri, S. J.; McLuckey, S. A. Parallel ion parking: Improving conversion of parents to first-generation products in electron transfer dissociation. *Anal. Chem.* **2005,** *77*, 3411–3414.
29. Chrisman, P. A.; Pitteri, S. J.; McLuckey, S. A. Parallel ion parking of protein mixtures. *Anal. Chem.* **2006,** *78*, 310–316.
30. Moradian, A.; Douglas, D. J. Mass selective axial ion ejection from linear quadrupoles with added octopole fields. *J. Am. Soc. Mass Spectrom.* **2008,** *19*, 270–280.
31. Stephenson, J. L.; McLuckey, S. A. Adaptation of the Paul Trap for study of the reaction of multiply charged cations with singly charged anions. *Int. J. Mass Spectrom. Ion Processes* **1997,** *162*, 89–106.
32. Mo, W.; Langford, M. L.; Todd, J. F. J. Investigation of 'ghost' peaks caused by nonlinear fields in the ion trap mass spectrometer. *Rapid Commun. Mass Spectrom.* **1995,** *9*, 107–113.
33. Franzen, J.; Gabling, R. H.; Schubert, M.; Wang, Y. In *Practical Aspects of Ion Trap Mass Spectrometry*, Vol. I; March, R. E.; Todd, J. F. J., Eds.; CRC Press: Boca Raton, FL, 1995;Vol. 1, p. 49–167.